

# Interpretation of Aeromagnetic and Radiometric Data of Potiskum and Its Environment, Chad Basin Nigeria

ABDULLAHI BABALE<sup>1</sup>, PROF. ABU MALAM<sup>2</sup>, DR. TAJUDEEN ADEEKO<sup>3</sup>

<sup>1, 2, 3</sup>University of Abuja

**Abstract-** Interpretation of geophysical data of aeromagnetic and radiometric sheets of Potiskum and its environments was interpreted. The depth and extend to magnetic basement, the lineament structures, the geothermal gradient, heat flow, Curie point depth and radiogenic heat production zones of the study area was investigated. The results revealed that the lineament structures revealed some trend of cracks that might be significant for minerals deposits across the study area. The source parameter imaging shows the shallow and deepest thick sedimentary rock which has the approximate values of -164.639 m (0.164639 km) and -2232.078 m (-2.23208 km). The shallow magnetic source depth (dark blue, blue and green) of estimated value of 164.639 m (0.164639 km), within the study area. The finding also revealed the Depth to Top Basement (Zt,) Depth to Centroid (Zo,) and the Curie Depth (Zb) with approximate average values of 1.6 km, 5.72 km and 9.85 km. The geothermal Gradients and Heat Flow average values of 66.22 0Ckm-1 and 165.55 mWm-2. The average geothermal gradient of 66.22 °C km-1. The results also revealed that, the computed sedimentary thickness (1.2 to 2.8 km) and the temperature at a depth of (55 to 65 0C/km), the areas like Mamudo, Fara-Fara, Dakasku, Bulakos, kusulwa, Bade, Potiskum have more potential for hydrocarbon generation and accumulation. The study also revealed the high radionuclides concentration of 238U, 232Th and 40K which might be associated with metamorphic rocks like granites and gneiss, while other parts that shows low nuclides concentration might be associated with sedimentary rocks such as shale, clay and limestone. High concentration of radiogenic heat has the highest occurrence around the study area.

**Indexed Terms-** Geothermal Gradient, Curie point, Sedimentary, Radiogenic.

## I. INTRODUCTION

Nigeria is enriched with different energy sources, specifically, it's Inland Basin. Unarguably, industrialization opportunities would cut down unemployment. Availability of difference sources of energy provide growth and national development. It would also eradicate poverty and reduces the level of insecurity. This research might add up to the existing projects. Concerning the problem of the Nigerian Power sector, the research will light up the prospect areas for geothermal energy resources. The Power Generation in Maiduguri, is suffering from gas (LNG) supply by GreenVille Energy. If geothermal energy resources properly harness, would cut-down the cost of Power Generation.

Water of warm springs in Akiri and Ruwan Zafi in Nigeria has the temperature of about 54°C, suggesting occurrence of some geothermal anomalies (Kwaya and Kurowska 2018)

The work is an attempt to investigate hydrocarbon and geothermal prospecting areas for economic potentials. Interpreting and analyzing a digital magnetics and radiometric data, might give estimated mean volumes of undiscovered and recoverable oil and gas resources. Combination of radiometric interpretation and magnetic data in the study area, might differentiate and characterize the region of sedimentary thickness and shallow basement.

### Stratigraphic Setting of Chad Basin

The Cretaceous Rift system of West and Central Africa extend for over 4000 km from Nigeria northwards into Niger and Libya and eastwards through southern Chad into Sudan and Kenya (Fairhead 2023). The Fika Formation is made up of blue-grey shales, with irregular limestone layers. Coniacian to Santonian age has been assigned to this formation. Overlying the Fika shale is the Gombe Formation. From outcrop and shallow borehole studies

the formation consists of rare basal conglomerate, grit, sandstone and clay. The stratigraphic unit representations in Chad Basin aged from Albian to recent (Ola, 2018). Deposition took place under varying conditions with each deposit representing one complete cycle of transgression and regression. This, has been divided into six formations based on the nature of sedimentary deposits within the depression. The divisions were named Bima, Gongila, Fika, Gombe, Kerri-Kerri and Chad formations (after Okosun 1995). The Nigeria Government recently commissioned integrated investigation that involve seismic, magnetic, geochemical, paleoclimatology, rock facies assessments, aerial photography, magnetic investigation, prospect of gravity and exploratory boreholes mainly in Cretaceous inland basins of Nigeria for geoscientists conduct (Ekwok et al., 2021). Then, the Bima Sandstone is conformably overlain by the Gongila Formation which is composed of calcareous shale and sandstones, deposited in a shallow marine environment (Yusif, *et al* 2022).

Ezekiel and Peter (2023) used spectrum analysis and empirical formula to interpret aeromagnetic data and also estimated the values of Curie point depth, geothermal gradient, and heat flow, then acquired regional and residual data, polynomial fitting to the high-resolution digital aeromagnetic data within Potiskum. The calculated depth to the centroid and the depth to the top boundary, the upward continued residual data processed to obtain the upward continued data, which was subjected to spectral analysis. The values obtained for depth to the centroid was between 10.50 and 11.50 km, the depth to the top was between 5.90 and 7.16 km, the depth to the Curie point was between 14.84 and 16.83 km, the geothermal gradient was between 34.462 and 39.083 °Ckm<sup>-1</sup>, and the heat flow was between 86.135 and 97.707 mWm<sup>-2</sup>. The Curie point depth revealed in the studied area indicates that the crust is thinning due to thermal upwhirling of magma and is moderately decreasing toward areas of volcanic activity that occurred in the area during the Tertiary Period.

The Geothermal gradient shown the moderate area temperature zone, which could likely result in partial thermal maturation of sediments and hence probable oil generation as time goes on with an increase in temperature. The research revealed that the geothermal gradient is proportional to the heat flow,

while the relationship between curie depth and heat flow is inversely linear. However, the analyzed data shown that the heat flow obtained from the studied area is sufficient to be utilized as a geothermal energy source. Therefore, geomagnetic anomalies, which are retrieved from magnetic survey data, can be utilized to study magnetic structures above the Curie point depth (Yaro et al., 2023). Tarshan et al. (2023) described the basic 2-D spectral analysis method, and they estimated the depth to the top of magnetized rectangular prisms ( $Z_t$ ) from the slope of the log power spectrum. Then, Ukwuteyinor et al. (2023) further calculated the depth to the centroid of the magnetic source bodies ( $Z_0$ ), and developed a method to estimate the bottom depth to the magnetic bodies ( $Z_b$ ) by using the spectral analysis method of Tarshan et al. (2023). considering the method presented by Geng et al. (2023), it was assumed that the layer extends infinitely in all horizontal directions.

Abdullahi *et al.* (2021) assessed the chad basin region using a High-Resolution aeromagnetic data of chad basin, with the method of spectral analysis and determined the depth to the basement. The results showed that depth to the deepest magnetic source ranged from 4503.9 m to 1948.3 m. The authors observed that NN, NE, and NW have less deep magnetic sources ranged from 1948 m to 2459.7 m. The deepest sources revealed at the major towns of interest which were Bidawa , Matsango , Yakiri and Fatara, and Katagum Bauchi state, which ranged from 2632.8 m to 4503.9 m. The deepest depth of the sedimentary unit was estimated at 4.5 km.

Ekundayo *et al.* (2021) determined using the vertically drilled Gaibu-1 Well for a total depth of 4620 m of dominantly siliciclastic detritus. They used recovered ditch cuttings, self-potential and gamma-ray logs from the Gaibu-1 for this studied work. Then, two hundred and ten (210) ditch cuttings acquired from the depth interval 1500 m to 4600 m of the well were then serially arranged and washed in distilled water to removed possible drilling mud/contaminants. The results revealed that the sediments consisted of predominantly sandstone, siltstone, sandy shale, and shale.

The sandstones ranged from fine-coarse, angular to sub-rounded, moderate to poorly sorted, and were texturally immature. Five (5) stratigraphic

subdivisions as Bima, the Yolde, the Gongila, the Fika (Upper, Middle and Lower members) and the Gombe formations identified. These suggested that the well penetrated Cenomanian – Maastrichtian (younger) successions.

Magama et al. (2022) evaluated aeromagnetic data of eastern Chad Basin. Use spectral block to estimate the depth to basement (Zt), centroid (Zo) and Curie point depth. The results obtained were depth to basement (Zt) with an average value of 5.96 km. The depth to centroid (Zo), with an average value of 11.08 km. The CPD with an average value of 16.20 km respectively. Musa et al., (2022), the analyzed high-resolution aeromagnetic data revealed the heat flow on the geothermal and hydrocarbon potential of Chad Basin. The estimated result of CPD and heat flow values, ranges from 11 km to 19 km and from 75 mW/m<sup>2</sup> to 125 mW/m<sup>2</sup> respectively. The depths to the magnetic sources range from about 0.1 km to about 5 km. The estimated result of heat flow in the study area, found to be sufficient for the economic exploitation of geothermal energy. The results revealed that, the study area is thermally matured for hydrocarbon generation. Stephen *et al.* (2022) estimated the sedimentary section of Chad Basin. After data collection from NGSAs, they use source parameter imaging, Euler deconvolution, MAGMAP, and 2-D GM-SYS extensions. Results of the sedimentary thicknesses from the source parameter imaging were approximately ranged from 286 m to 615 m, 695 m to 1038 m, and 1145 m to 5885 m for the thin, intermediate, and thick sedimentation, respectively. Euler deconvolution results showed 130 m to 917 m, intermediate from 1044 m to 1572 m, and thick from 1725 m to 5974 m of sedimentation.

Taiwo et al., (2022) estimated the sedimentary depth for hydrocarbon maturation and accumulation in Chad Basin, NE Nigeria. Used 2D magnetic structural and depth modelling. Source parameter imaging (SPI) was used to determine depth to geophysical features. SPI result indicates that the thickness of the sedimentary beds ranges from 1.02 km to 5.55 km, with a maximum thickness of about 3.0 km. The 2D magnetic depth taken from seven profiles on the RTE-TMI map in the area revealed significant anomalies. Lithological boundaries and thickness of sediments ranges from 1.0 km to 11.5 km. These shows that, thickness of

sediments of 3.0 km to 11.5 km is sufficient for Chad Basin hydrocarbon maturation and accumulation.

## II. MATERIALS AND METHODS

Aeromagnetic and Radiometric data from Nigerian Geological Survey Agency (NGSA) that covered Potiskum and its environment (86\_POTISKUM) sheet. The aeromagnetic data were acquired using a 3 x Scintrex CS2 caesium vapour magnetometer by Fugro Airborne Surveys between 2007 and 2009. The airborne magnetic survey was flown at a terrain clearance of 80 m along flight lines spaced 500 m apart. The Potiskum aeromagnetic data were recorded in digital form (X, Y, Z text file) after removing the geomagnetic reference field (IGRF). The X and Y represent the longitude and latitude of Potiskum in meters, while the Z represents the magnetic field intensity measured in nanotesla. The data obtained from the study area were during a nationwide survey to facilitate hydrocarbon and solid mineral exploration in Nigeria. International geomagnetic reference field was corrected and the total magnetic intensity ( $TMI = Reg. + Res.$ ) data of the study area was reduced to magnetic pole (RTP) using geomagnetic inclination of  $-11.595$  and declination of  $2.097$  (derived from IGRF 2005).

The methods used for the analysis of the collected data sheets from NGSAs are:

Analytical signals;  
Source Parameter Imaging (SPI) for depth estimation. Revealing areas of shallow and deep magnetic source. Depth estimates are calculated using the reciprocal of local wavenumber, given as:

$$Depth = \frac{1}{K_{Max}} \quad (1)$$

where,  $K_{Max}$  is the maximum value of K over the magnetic source body.

Spectral Analysis was used for Curie point depth, Geothermal gradient and Heat flow. FFT algorithms is made into data processing program of Microsoft Excel and analyze spectral lines of waveforms of geophysical data. The magnetic data was spread into spaced grid of cells in a stated coordinate system, then

the magnetic data converted into radial energy spectrum for every block of cell. Then, evaluated the average radial energy spectrum and a graph of energy against frequency was plotted using Excel chart wizard;

$\frac{\ln P(k)^{1/2}}{k}$  against  $k$ , from a slope of the longest wavelength (low frequency),  $Z_o$  the centroid of the magnetic source is estimated by fitting line via a lower- wave number part of the radially average frequency power spectrum.

$\ln(p(k)^{1/2})$  against  $k$  ( $y$ ) the second longest wavelength (high frequency),  $Z_t$  the upper bound of magnetic source is estimated by fitting a line through higher-wave number part of the radially average power spectrum.

Then, the Basal depth  $Z_b$  of the magnetic source is calculated from the equation  $Z_b = \frac{2Z_o - Z_t}{2}$   $Z_b$  is assumed to be Curie point.

The Geothermal Gradient is calculated from the equation

$$\frac{dT}{dz} = \frac{T_c - T_s}{Z_b} = \frac{580^\circ\text{C} - T_s}{Z_b} \quad (3)$$

where  $T_s$ , is the surface temperature assume to 0. Then, the quantity of heat  $q$  as the heat flow and  $k$  the coefficient of thermal conductivity, the values obtained by this equation;  $q = k \left(\frac{dT}{dz}\right)$ . The thermal conductivity of a value  $2.5 \text{ Wm}^{-1} \text{ }^\circ\text{C}^{-1}$  as an average value of igneous rocks was used as standard.

Center for exploration technique (CET) grid analysis of Oasis Montaj was used to examine the texture of an image along ridges which identified linear discontinuities, edge detection and structural complexity for lineaments extraction;

The magnetic data collected were analyze using filters such as Total Magnetic Intensity to reveal the large geologic features, regional TMI Map. The regional magnetic map produced by the use of upward continuation of total magnetic intensity map to reveal more details of local geologic features, analytic signal to reveal the extent of magnetic signals, Lineament

Map and Source Parameter Imaging (SPI) to reveal the fracture zones and magnetic depth. Applied a stripping correction derived from the calibration of data and also the application of height attenuation corrections by Nigerian Geological Survey Agency (NGSA). The procedure determines the observed count rates distribution of their concentrations. A minimum curvature of Oasis Montaj was used to produce an enhanced radiometric distribution of the count rate, and a ternary image of potassium, thorium and uranium. Then, ternary image was assigned red, green and blue colors. Radioactive heat production from radiometric data is given according to (Salem and

Fairhead, 2011) by the expression:  
 $A(\mu\text{W}/\text{m}^3) = \rho(0.0952C_U + 0.0256C_{Th} + 0.0348C_K)$  (4)

where,

$A$  is radiometric heat (in  $\mu\text{W}/\text{m}^3$ )  
 $\rho$  is density of rock in  $\text{kg}/\text{m}^3$   
 $C_U$ ,  $C_{Th}$  and  $C_K$  are the concentrations of uranium, thorium and potassium (in ppm and %) respectively. The concentration of radiogenic elements is from the radiometric map covering the study area.

### III. RESULTS

The aeromagnetic maps interpreted as magnetic responses in the subsurface geological bedrock over the study area. Bi-directional gridding method was used to produce the Total magnetic intensity (TMI) anomaly grid (figure 1). The technique used was to separate the effect of local magnetic field of the study area from the regional field.

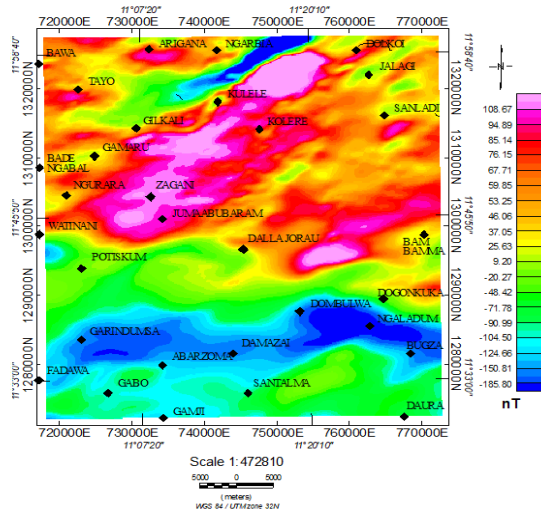
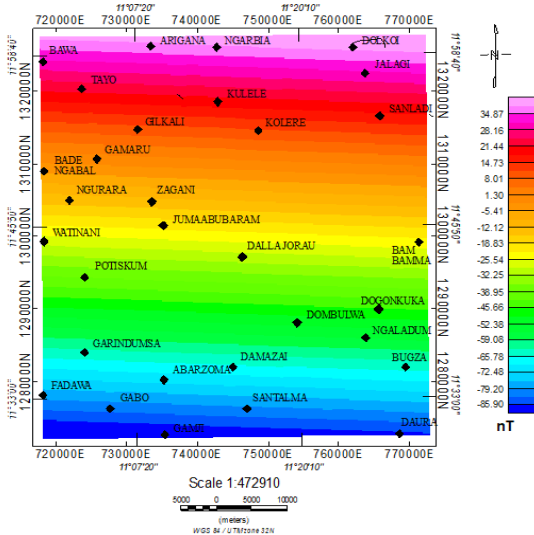


Figure 1: Total Magnetic Intensity of the Study Area

This allow residual interpretation of aeromagnetic data of shallower geologic formation. It was carried out for the depiction of deep-seated magnetic anomalies which covers the study area (figure 2).

The regional Magnetic Intensity Map (Figure 2) is divided into five major intensities such as; very high, high, moderate, low and very low that has the values that range from -85.90 – 34.87.



The residual map (figure 3) revealed the effect of local magnetic field variation from the regional field, and to help for residual interpretation of aeromagnetic data of

shallow geophysical signals that may have exploration significance. The residual map, used to determine a localized field effects and structures of importance for mineral exploration in the study area. Where the regions of higher magnetic intensities are Zagam, Juma'a/Bubaram, Dalla Jauro and Dogonkuka. The moderate regions are Kolere, Kulele, Bam-Bamma, Potiskum, Bade-Ngabal. The regions of lower intensities are Garindumsa, Damazai, Abarezoma, Dumbulwa, Bugza and Ngalda.

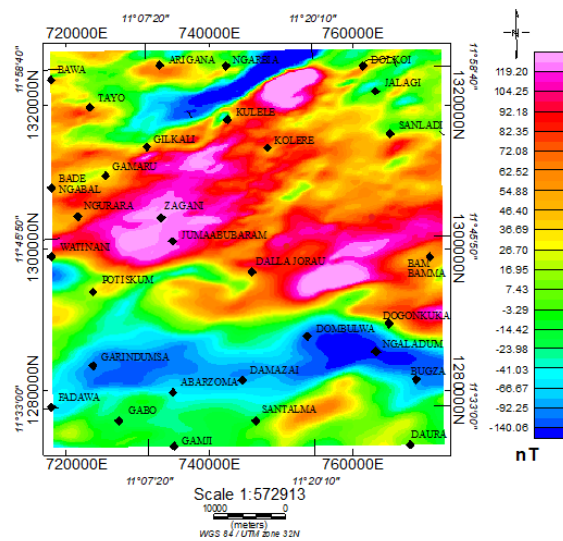


Figure 3: Residual Map of the Study Area

The areas of a strong positive magnetic anomalies might be high concentration of magnetic susceptibility minerals. While the areas of lower magnetic, has a lower susceptibility minerals. Which correspond to the work of Ayigun *et al.*, 2022

The lineament magnetic structures (figure 4) (mineral veins) and structural contacts. The lineament map indicates many densely populated contacts in the north central, and the lineament trends interconnected with each other, and trending EW with dense fractures that may be potential source of minerals deposits in the region. But at the south central, only few fractures observed. The geological map of the study shows presence of Gritty clay, sand, sandy clay and mudstones, blue-black shale, limestone and gysiferous. Therefore, fractures in the lineament

map signified minerals with rock-bearing the above characteristics.

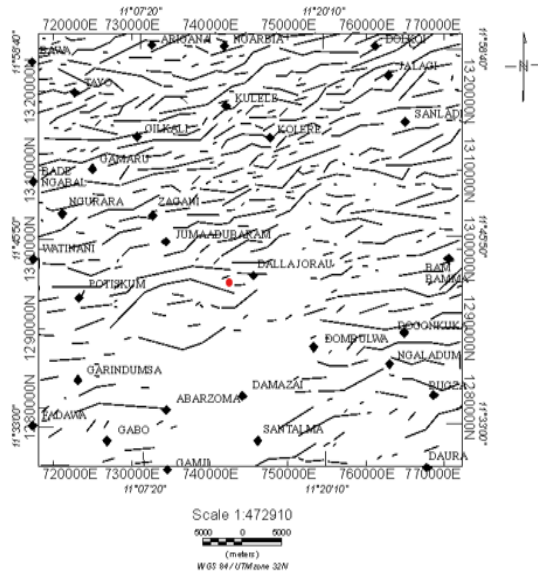


Figure 4: Lineament Map of the Study Area.

Source Parameter Imaging (Figure 5). The result of source parameter imaging shows regions of shallow and deep magnetic sources which were interpreted as sedimentary depth. The shallow magnetic sources, predominantly located within the central and the northern part of the study area.

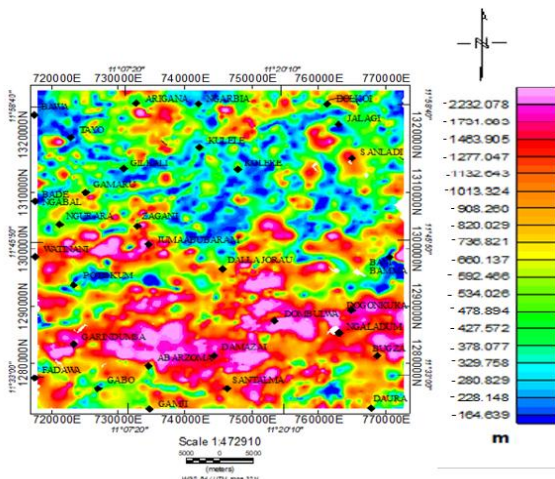


Figure 5: Source parameter imaging

The Spectral Blocks of the Study Area is divided into 9 blocks of equally spaced grid of cells. Stated in a coordinate system of radial energy spectrum for every

block of cell. The spectral block of the study area figure 6 shows 1 to 9 blocks, with values that ranges from -140.05 to 119.203 nT around the study area

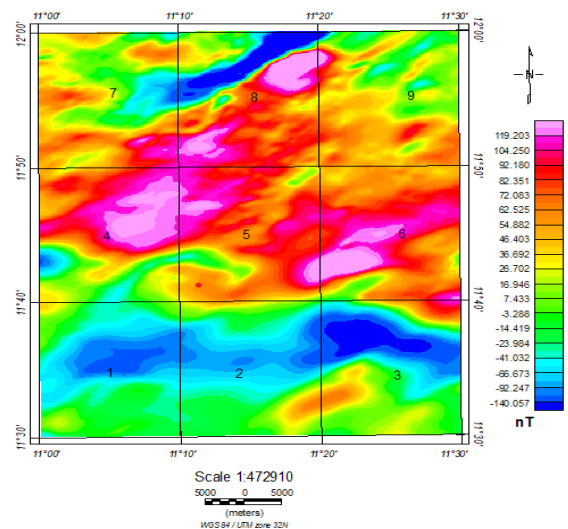


Figure 6: Spectral Blocks of the Study Area

A graph of energy against frequency was plotted. The Spectral Plot of the Study Area revealed that the longest wave length (low frequency) has a  $Z_0$  an average value of 5.72 km and the second longest wave length (high frequency)  $Z_t$ , has an average value of 1.6 km.

Table 1 shows the depth values obtained from the spectral analysis plot. The average values of the heat flow ranges from 109 to 233.83  $mWm^{-2}$  with an average of 165.55  $mWm^{-2}$  in. The contour Map revealed the deeper depth of the study area as shown in figure (9 – 10). The contour map of the basement depth  $Z_t$  is thicker in the southwest (SW) of the study area around.



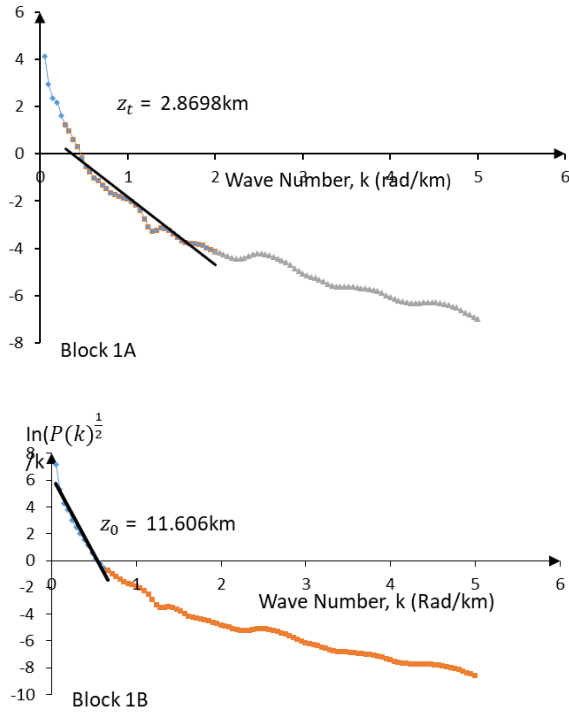


Figure 7: Spectral Plot of the Study Areas

Table 1: Estimated Depth to the top ( $z_t$ ), Depth to the centroid ( $z_0$ ), Curie depth ( $z_b$ ), Geothermal gradients (GTG) and Heat flow (HF) for 9 blocks in the study area.

Block	Longitude (Degree)	Latitude (Degree)	$z_t$ (km)	$z_0$ (km)	$z_b$ (km)	GTG ( $^{\circ}\text{C km}^{-1}$ )	HF ( $\text{mWm}^{-2}$ )
1	11.0835	11.5835	2.8698	11.606	20.3422	28.51	71.28
2	11.2500	11.5835	2.0022	7.6071	13.212	43.90	109.75
3	11.4165	11.5835	1.6604	5.3517	9.043	64.14	160.35
4	11.0835	11.7500	1.2261	4.8119	8.3977	69.07	172.68
5	11.2500	11.7500	1.3619	3.7815	6.2011	93.53	233.83
6	11.4165	11.7500	1.2516	4.4254	7.5992	76.32	190.80
7	11.0835	11.9165	1.4382	4.5095	7.5808	76.51	191.28
8	11.2500	11.9165	1.3473	4.3427	7.3581	78.82	197.05
9	11.4165	11.9165	1.2349	5.0671	8.8993	65.17	162.93
<b>Average</b>			1.6	5.72	9.85	66.22	165.55

Therefore, the Curie Depth of the Study Area corresponds to the Depth to Centroid in the Study area. The areas of shallower depth also correspond to each other. The calculated geothermal gradient from the table ranges from 28.51 to 93.53  $^{\circ}\text{C km}^{-1}$  with an

average value of 66.22  $^{\circ}\text{C km}^{-1}$  (Table 1). The anomalous high temperature gradient of the region of lower geothermal gradient ranges from 28.51 to 43.90  $^{\circ}\text{C km}^{-1}$ .

The calculated heat flow values ranges from 109 to 233.83  $\text{mWm}^{-2}$  with an average value of 165.55  $\text{mWm}^{-2}$  in (Table 1). Figure 9 showed the deepest values are found around Fadawa and Langawa (2.6 to 3 km), and shallower depth found around Fara Fara, Mamudo, Bade, Alaraba (1.2 to 1.7) in the study area.

Figure 8, the Curie point depth reveal the deepest (red color) depth with values of 18 to 20 km<sup>2</sup> (Fadawa and Langawa). The shallow (blue color) has a values of 8 to 10 km<sup>2</sup> (Santalma, Dakasku, Fara-Fara, Mamudo, Bade, Alaraba, Nangere and Abakire). While the shallowest towns are Aigada, Bula, Damagum, DogonKuka and Gaba.

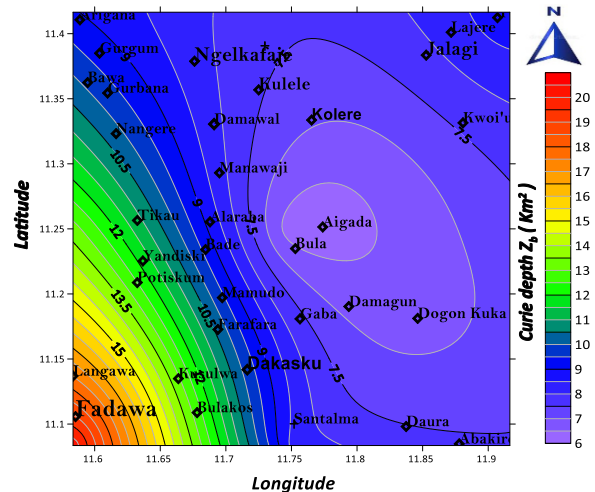


Figure 8: Curie Depth Of the Study Area

Figure 9, the geothermal gradient shows the region of high and low geothermal energy anomalous temperature. But the regions for the probable geothermal energy resources which has an anomalous values of 40 to 65  $^{\circ}\text{C / Km}$  (Bulakos, Kusulwa, Potiskum, Yandiski, Tikau and Nangere), indicate the possibility of Hydrocarbon generation in the study area.

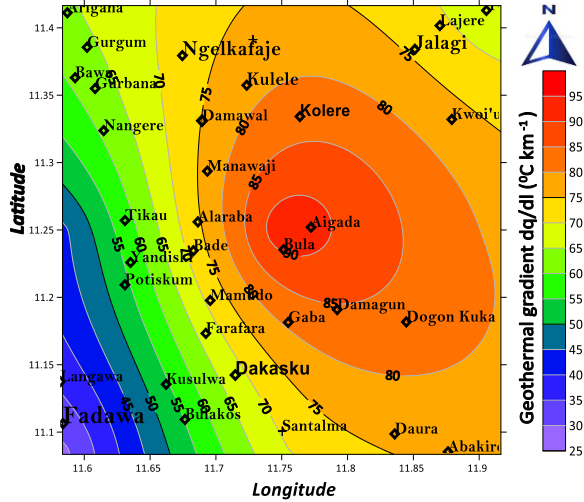


Figure 9: Geothermal Gradient Map of Study Area

The heat flow values, figure 10 show a region of an anomalous high temperature and the lowest temperature. Heat flow values in the study area increases with decreasing Curie point depth. Heat flow values ranges from 70 to 240 mWm<sup>2</sup>.

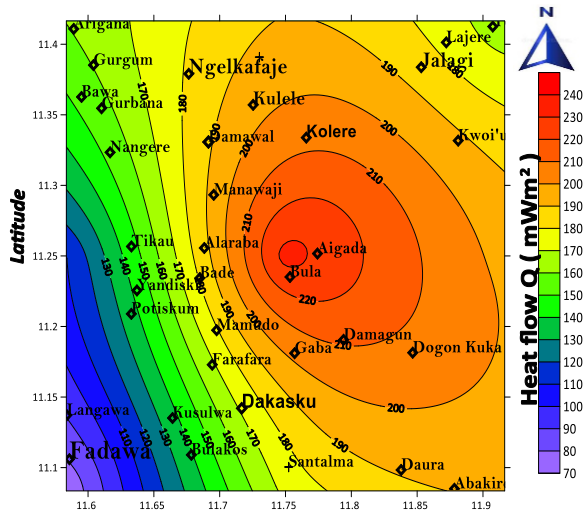


Figure 10: Heat Flow of the Study Area

The depth to centroid, figure 11 shows the region of deepest basement and the region of shallower basement in the study area. Depth to centroid Z<sub>0</sub>, has a values that ranges from 3.5 to 12 km in the study area.

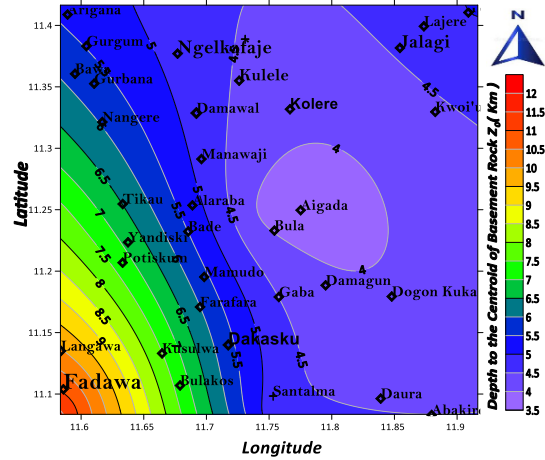


Figure 11: Depth to Centroid of Basement Rock

Figure 12, the depth to top of basement shows a sedimentary thickness of about 1.2 to 3 km.

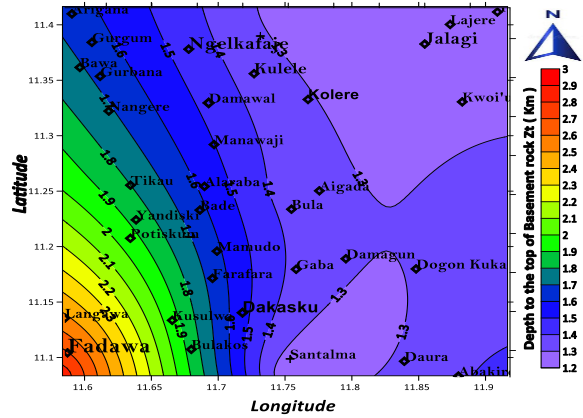


Figure 12: Map of Depth to Top of Basement Rock

The Radiometric Method of the Study Area

The maps produced various rocks with different concentrations of the natural radionuclides. The Potassium Map shows the areas of high percentages like Daura, Gamji, Ngalda, Bugza and Dogonkuka which largely trended NE – SE and few signal spread around other regions. Low signals of percentage were observed around NW- SW and some part of NE and SE region.



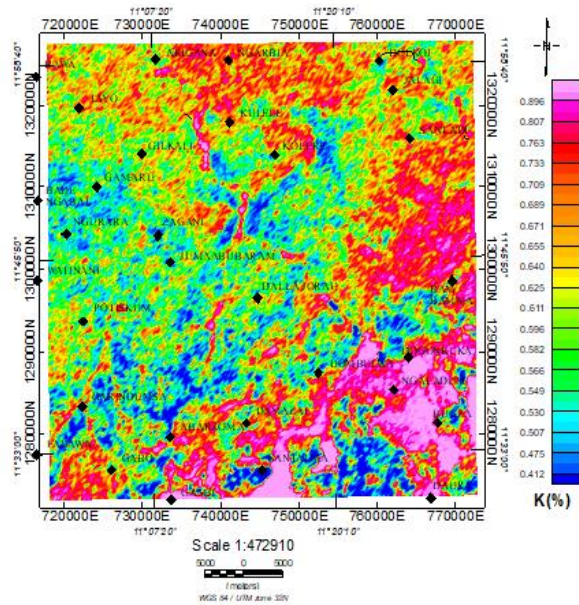


Figure.13: Potassium Map of the Study Area

Figure 14 shows Thorium (eTh) concentration map in parts per million (ppm) with the high concentration of eTh range to rocks bearing rich thorium minerals within the study area. eTh radiation shown in the study area clearly reveal the variation in lithology, fault, regional lineament, as well as the degree of signature for weathering and rich regions in thorium bearing-minerals.

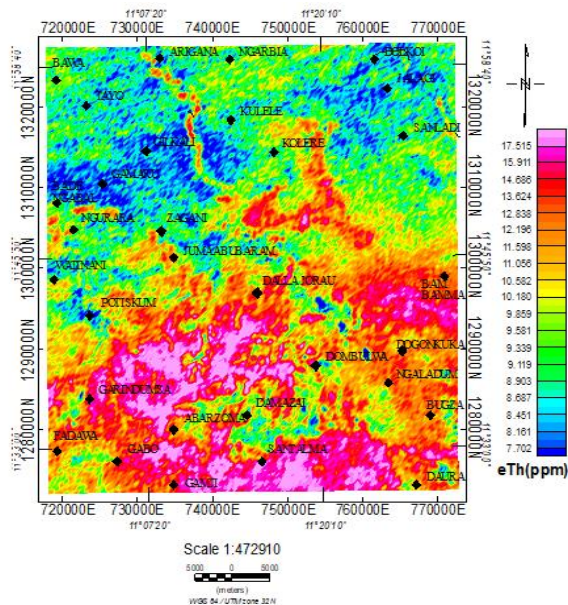


Figure 14: Equivalent Thorium Map of the Study Area

The equivalent Uranium (eU) Map of the Study Area in figure 15 shows that the highest concentration of Uranium is in the south-south west, south-south east and the extreme end of the southern parts of the study area. While the lower equivalent concentration is located at north-north east, north-north west and the extreme north.

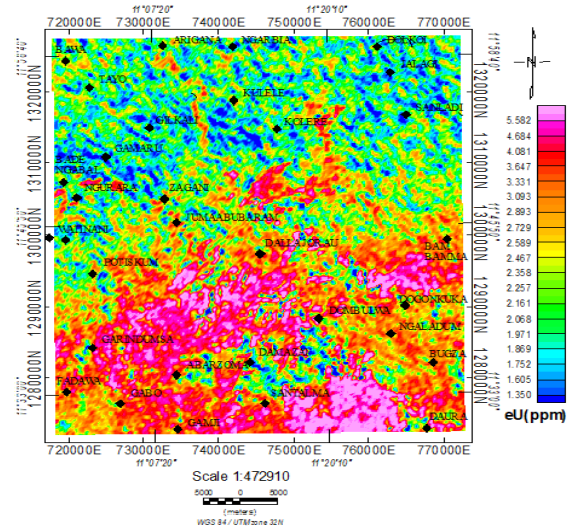


Figure 15 Equivalent Uranium (eU) Map of the Study Area

The radiometric data in figure 16 is ternary image of the study area. The map, combined the signals intensities of Potassium (K), Thorium (eTh), and Uranium (eU) concentration. Represented in red, green, and blue color respectively. The three major intensities of radiometric data in the study area, revealed the behavior of three radiogenic elements of K, eTh and eU across the study area.

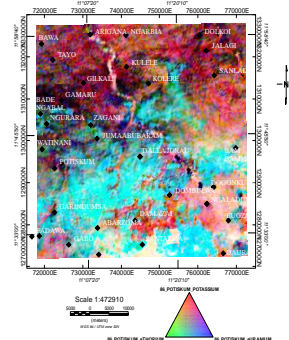


Figure 16: Ternary Image of the Study Area

## IV. DISCUSSION

The low frequency of the magnetic signature in the Total Magnetic Intensity map, Regional map and Residual map dominated the southern part of the study area. This implies high depth to basement, hence, the deep seated magnetic bodies. While the high magnetic signature indicate shallow depth, hence, might be intrusion or near surface magnetic bodies. Rabo *et al.*, (2021) observed that the high magnetic anomaly in most part of Chad Basin is as a result of intrusion of magnetic bodies. The high or strong positive anomalies likely indicates a higher concentration of magnetically susceptible minerals. While lower signals, shows low susceptibility minerals. This correspond to work of Ayigun *et al.*, (2022).

The lineament structure across the study area revealed some cracks around North central to North-North-West and lower cracks are located around North-East of the study area. The revealed anomalies within Ngarbia and Kulele corresponds to the magnetic low intensity in the residual grid map of the study area. These anomalies, suggest occurrence of ferruginous material like ironstone in large quantity (rock bearing minerals from the geology map). These ironstone rock bearing minerals were also manifested around North of Potiskum, Dumbulwa, Dogon Kuka, Ngaladum, Bugza and around the southern part of Watinani.

The result of source parameter imaging (Figure 5) shows regions of shallow and deep magnetic sources. Interpreted as thick sedimentary cover with deep magnetic sources. The southern parts, are interpreted as low magnetic susceptibility coming from sandstone and clay rich minerals. The deepest rock (magenta and red) with estimated value of -2232.078 m (-2.23208 km). Located around Jumma'a Bubaram, Zagam, Dumbulwa, DogonKuka Garindumsa. Closely corresponds to the values obtained from Top to Basement  $Z_t$  (1.2 to 3 km) in the study area. The shallow magnetic source depth (dark blue, blue and green) of estimated value of 164.639 m (0.164639 km), predominantly located within the central and the northern part of the study area around Bambamma, Jalagi, Kulele, Gilkali, Bawa, Potiskum and Bade Ngabai.

The Depth to basement (figure 12) ( $Z_t$ ) found in this study ranges from 1.2 to 3 Km. Depth to Centroid of basement rock (figure 8) showed values that ranges from 3.5 to 12 Km. The calculated geothermal gradient (figure 9) ranges from 28.51 to 93.53 °C km<sup>-1</sup> with an average value of 66.22 °C km<sup>-1</sup> (Table 1). The anomalous high temperature gradient, is the region of lower geothermal gradient. Ranges from 28.51 to 43.90 °C Km<sup>-1</sup>. The heat flow values range from 109 to 233.83 mWm<sup>-2</sup> with an average value of 165.55 mWm<sup>-2</sup> in (Table 1). Figure 10 shows that the highest heat flow values are found around the central part, North-North to North-West, of the study area. The moderate is at Kusulwa, Nangere, Tikau, Bulakos. The lowest values are located at the extreme South-West of the study area (Fadawa and Langawa).

The high geothermal energy region is characterized by anomalous high temperature gradient and heat flow; therefore, the expectation is that, geothermally active regions will be associated with shallow Curie point depth. Nwankwo and Ekine (2009) from their work, geothermal gradient within the range of 30–44 °C km<sup>-1</sup> and the average value of 34 °C km<sup>-1</sup> from Geothermal Gradients within Chad Basin, Nigeria,

The calculated Curie point Depths, Geothermal Gradient and heat flow values obtained by Nwobodo (et. al, 2018) ranged from 10.220 to 22.721 km, 25.527 to 56.751 °C km<sup>-1</sup> with an average value of 38.517 °C km<sup>-1</sup> and 63.818–141.878 mW m<sup>-2</sup>, respectively. The areas of geothermal anomalies with gradients above 50 °C km<sup>-1</sup> revealed in this study may be favorable for geothermal energy exploration around the region for generation of electricity. This also agreed with the work of Kurowska and Schoeneich (2010), found that the geothermal gradient above 50 °C km<sup>-1</sup> may also be favorable for geothermal energy exploration for electricity generation in Nigeria. The average geothermal gradient of 66.22 °C km<sup>-1</sup> revealed the hydrocarbon generation possibility around the study area, which corresponds with the work of Nwankwo and Ekine (2009) on the geothermal gradient estimation within the Chad Basin, Nigeria. Their work showed that the sediments with greater geothermal gradients of 30 to 44 °C km<sup>-1</sup> mature earlier (low oil window) than the ones with smallest geothermal gradient values. But the result obtained didn't correspond with result obtained by

Ezekiel and Peter (2023). Their results of depth to the centroid was between 10.50 and 11.50 km, the depth to the top boundary was between 5.90 and 7.16 km, the depth to the Curie point was between 14.84 and 16.83 km. The geothermal gradient was between 34.462 and 39.083 °Ckm<sup>-1</sup>.

A greater geothermal gradient, the range of the oil window will be quite narrow. While low geothermal gradient causes the first formation of oil to start at fairly deep subsurface levels, though, it makes the oil window reasonably wide. However, the computed sedimentary thickness (1.2 to 2.8 km) and the temperature at a depth of (55 to 65 °C/km), the areas like Mamudo, Fara-Fara, Dakasku, Bulakos, kusulwa, Bade, Potiskum have more potential for hydrocarbon generation and accumulation.

The interpretation of radiometric data within the study area revealed the concentration distribution of the three radioelements of Potassium (K), Thorium (Th) and Uranium (U). The result obtained, delineated and characterized for the mineralization prospects around the study area.

The potassium distribution around the study areas with high percentages are Daura, Gamji, Ngalda, Bugza and Dogonkuka are largely spread (red-orange) NE – SE (magenta-pink) and few signals spread around other regions. Low signals were also observed around (dark-blue and light-blue) NW- SW and some part of NE and SE region (yellow) of the study area.

The thorium (eTh) distribution show high (magenta), moderate (pink-orange), moderately low (yellow-green) and low (dark-blue-blue) eTh values. The high-density (cardinal red-blue) regions are located at SW and SE, the moderately high (yellow-white) spread across SW, SE, NE and NW within the area.

The equivalent Uranium (eU) around south-south to extreme south of the study area revealed that Dombulwa, Damazai, Daura and Ngurara has a higher equivalent density, Bade Ngabal, BamBamma, Bugza, Dallajorau, Dogonkuka, Fadawa, Gabo, Santalma, Ngaldum, and Watinani has moderate concentrations and low-density areas are Bawa, Kolere, Kulele, Potiskum, Zagam.

Comparing the radiometric heat in the study area with the geology of the area, those areas with high geothermal heat flow and high radiogenic heat concentrations are those covered by basement complex, Gritty clay, sandstones and shale.

Parts of these study area that shows high radionuclides concentration of <sup>238</sup>U, <sup>232</sup>Th and <sup>40</sup>K 5.582ppm, 17.515ppm and 0.896% might be associated with metamorphic rocks such as granites and gneiss, while other parts that shows low nuclides concentration might be associated with sedimentary rocks such as shale, clay and limestone (Obi, 2014).

The ternary map (Figure 16) shows the relative abundance of U, Th and K in the study area. The map shows that Uranium is most abundant in the study area, especially at the southern parts of the study area followed by the combination of all radionuclides especially around the central northeastern part of the study area. The combination of eTh and eU concentration is at the central south, south-south-west and the extreme south of the study area. The areas with high eU and eTh are considered anomalies that could be significant for radioelement mineralization, while areas with low eU and eTh might be considered anomalies for potential hydrocarbon. High concentration of radiogenic heat has the highest occurrence around the study area.

These areas are the hot spots which are potential geothermal areas. The areas of high radiometric heat concentration correspond with the areas with low Curie point depth, high geothermal gradient and high geothermal heat flow. Places like Aigada, Bula, Damagum, Alaraba, Kolere, Dogon Kuka, Daura, Manawaji, Kolele, might be favorable for geothermal energy resources. While the result of SPI and Z<sub>t</sub>, shows that the basement might host hydrocarbon.

## CONCLUSION

The lineament structures revealed some cracks that might be associated to minerals deposits. The results of source parameter imaging shows the shallow and deepest thick sedimentary rock, with approximate values of -164.639 m (0.164639 km) and -2232.078 m (-2.23208 km). The finding also revealed the Depth to Top Basement (Z<sub>t</sub>), Depth to Centroid (Z<sub>o</sub>) and the

Curie Depth ( $Z_b$ ) with approximate average values of 1.6 km, 5.72 km and 9.85 km. also, geothermal Gradients and Heat Flow have the average values of  $66.22\text{ }^{\circ}\text{Ckm}^{-1}$  and  $165.55\text{ mWm}^{-2}$ . Then, the computed sedimentary thickness (1.2 to 2.8 km) and the temperature at a depth of (55 to  $65\text{ }^{\circ}\text{C/km}$ ), the areas like Mamudo, Fara-Fara, Dakasku, Bulakos, kusulwa, Bade, Potiskum have more potential for hydrocarbon generation and accumulation.

The study also revealed that, the high radionuclides concentration of  $^{238}\text{U}$ ,  $^{232}\text{Th}$  and  $^{40}\text{K}$ , might be associated with metamorphic rocks like granites and gneiss. While the low nuclides concentration might be associated with sedimentary rocks such as shale, clay and limestone.

#### REFERENCES

- [1] Abdullahi H., Bello Y. I., Chifu E. N., Maharaz M. N., Ahmad A., Nasiru B., Auwal I., Nasir Y., and Ibrahim A. (2021). Depth to Basement Using Spectral Analysis of Aeromagnetic Data over Determination Azare Chad Basin. *Dutse Journal of Pure and Applied Sciences (DUJOPAS)*, Vol. 7 No. 4b.
- [2] Ayigun S., Hamid K. Y. nad Omoniyi O. T. (2022) Review: Spectral Analysis of aeromagnetic data. *International Research Journal of Pure and Applied Physics*, (9) 1, 1- 11.
- [3] Ekundayo J. A., Bamidele S. O., Peter S. O. (2021). Late Cretaceous Palynostratigraphy of Subsurface Sediments of Southern Bornu Basin, Nigeria: Implications for Depositional Environments and Palaeoclimate.
- [4] Ekwok, S. E., Akpan, A. E., Ebong, E. D., Eze, O. E., (2021). Assessment of depth to magnetic sources using high resolution aeromagnetic data of some parts of the Lower Benue Trough and adjoining areas, Southeast Nigeria. *Advances in Space Research*, 67(7), 2104-2119.
- [5] Kamureyina E. Yohanna P. (2023) Curie Point Depth from Spectral Analysis of Magnetic Data in Potiskum and Environs, Yobe State, Nigeria *Dutse Journal of Pure and Applied Sciences (DUJOPAS)*, Vol.9  
[Nohttps://dx.doi.org/10.4314/dujopas.v9i4a.3](https://dx.doi.org/10.4314/dujopas.v9i4a.3)
- [6] Fairhead, J.D. (2023). The Mesozoic West and Central Africa Rift System (WCARS) and the older Kandi Shear Zone (KSZ): Rifting and tectonics of North Africa and South America and fragmentation of Gondwana based on geophysical investigations. *Journal of African Earth Sciences*, 199, p.104817
- [7] Geng, M., Ali, M.Y., Fairhead, J.D. and Saibi, H., (2023). The Curie depths of the United Arab Emirates: Implications for regional thermal structures and tectonic terranes. *Tectonophysics*, 848, p.229721.
- [8] Kurowska E., Schoeneich K. (2010). Geothermal Exploration in Nigeria. In: Proceedings of the world geothermal congress 2010 Bali, Indonesia, pp 25–29.
- [9] Magama A. A., Sanusi Y. A., Mikailu A. , Baban K. Y. and Isma'il U. I. (2022). Evaluation of Sedimentary Thickness and Curie Point Depths in The Eastern Part of Bornu Basin, North-Eastern Nigeria. *Dutse Journal of Pure and Applied Sciences (DUJOPAS)*, Vol. 8 No. 3b September
- [10] Musa O. A., Sesan C. F., Augustine A., Olaide H. (2022.), Magnetically inferred regional heat flow and geological structures in parts of Chad Basin, Nigeria and their implications geothermal and hydrocarbon prospects March 2022 *Journal of Petroleum Science and Engineering* 213:110388 213:110388.
- [11] Nwankwo CN, Ekine AS, Nwosu LI (2009). Estimation of the Heat Flow Variation in the Chad Basin Nigeria. *J. Appl. Sci. Environ. Manage.* 13(1): 73-80.
- [12] Nwobodo A. N., Ezema P.O., Ugwu G.Z (2018). Determination of the Curie point depth, Geothermal Gradient and Heat flow of Guzabure and its Environs, Chad Basin, Nigeria, using aeromagnetic data. *Int JSci Eng Res* 9(3):1876–1890
- [13] Obi D.A., Menkiti R.C., Okereke C.S. (2014) Aeromagnetic Anomalies Modeling and their Tectonic Implications in the Middle Benue Trough, Nigeria. *Journal of Environment and Earth Sciences*; 4(7): 1-11.

[14] Okosun EA (2000). A preliminary assessment of the petroleum potentials from Southwest Chad Basin, Nigeria. *Journal of Geology* 2: 40-50.

[15] Ola, P.S. (2018) Source Rock Evaluation of the Shale Beds Penetrated by Kinsar-1 Well, Se Bornu Basin, Nigeria. *Open Journal of Geology*, 8, 1056-1068. <https://doi.org/10.4236/ojg.2018.811064>

[16] Rabo Y., Bonde D. S., Bello A. and Abubakar I. (2021). Estimation of Basement Depth of Eastern Part Sokoto Sedimentary Basin Northwestern Nigeria. 2(1), 22 – 20.

[17] Solomon N. Y., Lucky O. I., Ovyé M. Y., Yusuf I., Asabe Y. K. (2022) Imaging Magmatic Intrusions using Derivatives of High-Resolution Data Over the Nigerian Sector of the Chad Basin. Published by Elsevier B.V. on behalf of African Institute of Mathematical Sciences/Next Einstein Initiative.

[18] Stephen E. E., Ogiji. I. M. A., Anthony E. A., Ahmed M. E., Chika H. U. Kamal A. and David G.O. (2022). Depth Estimation of Sedimentary Sections and Basement Rocks in the Bornu Basin, Northeast Nigeria Using High-Resolution Airborne Magnetic Data

[19] Tarshan, A., Azzazy, A.A., Mostafa, A.M. and Elhusseiny, A.A., (2023). Determination of Curie Point Depth and Heat Flow Using Airborne Magnetic Data over the Kom-Ombo and Nuqra Basins, Southern Eastern Desert, Egypt. *Geomaterials*, 13(4), pp.91-108.

[20] Taiwo A., Salako K. A., Akingboye A. S., Muztaza N. M., Alhassan U. D., Udensi E. E (2023). Reconstruction of the subsurface crustal and radiogenic heat models of the Bornu Basin, Nigeria, from multi-geophysical datasets: Implications for hydrocarbon prospecting

[21] Ukwuteyinor, B.U. and Ezeh, C.C., (2023). Evaluation of depth to basement, Heat Flow, and Lead-Zinc mineralization from analysis of aeromagnetic data in some parts of Southern Benue Trough. *Evaluation*, 13(2).

[22] Yaro, U.Y., Abir, I.A. and Balarabe, B. (2023). Determination of Curie point depth, heat Flow, and geothermal gradient to infer the regional thermal structure beneath the Malay Peninsula

using de-fractal method. *Arabian Journal of Geosciences*, 16(1), p.84

Appendix

